Orientation tuning and synchronization in the hypercolumn model

Sang-Gui Lee
Nonlinear & Complex Systems Laboratory, Pohang University of Science and Technology (POSTECH), Pohang, Korea

Shigeru Tanaka
Laboratory for Visual Neurocomputing, Brain Science Institute (BSI), The Institute of Physical and Chemical Research (RIKEN), Wako-shi, Saitama, Japan

Seunghwan Kim
Nonlinear & Complex Systems Laboratory, Asia Pacific Center for Theoretical Physics (APCTP), Pohang University of Science and Technology (POSTECH), Pohang, Korea

(Received 2 March 2002; revised manuscript received 12 September 2002; published 30 January 2004)

The orientation selectivity in the firing rate of neurons is one of the most well-known properties of neurons in the primary visual cortex. To understand the dynamical mechanism of the orientation tuning, we introduce a biologically plausible network for a hypercolumn and investigate dynamical responses of its columnar activities. Numerical simulations show that the spike activities between excitatory cells in the same column exhibit strong synchronization and sharp orientation selectivity. The tuning curves for the synchronized activities also show orientation selectivity similar to those for the firing rate. The comparison between the two tuning curves for the firing rate and the synchronized activities suggests that the orientation selectivity is strongly correlated with the synchronized activities. We find from the analysis of columnar activities that the orientation selectivity depends strongly upon the inhibitory coupling strength and the synchronization upon the excitatory coupling strength. In particular, we find that at appropriate coupling parameters both sharp orientation selectivity and maximal synchronization can be achieved. This suggests the importance of the balance between the excitatory coupling and the inhibitory coupling in the primary visual cortex for visual information processing.

DOI: 10.1103/PhysRevE.69.011914 PACS number(s): 87.19.La, 05.45.Xt, 05.10.−a

I. INTRODUCTION

So far, one of the most important questions regarding neural response properties in the primary visual cortex has been how the neurons become selective to a visual stimulus orientation [1,2]. In other words, this question is how the orientation selectivity emerges in the visual cortex in spite of weak orientation selectivity of neurons, if any, in the lateral geniculate nucleus (LGN). Several models to address this question have been proposed; however, the problem still remains controversial. In the conceptual model proposed by Hubel and Wiesel [3], the geniculocortical inputs are assumed to give the main contribution to the emergence of orientation selectivity; that is, the cortical neurons obtain orientation selectivity from the elongated patterns of converging thalamic inputs. An alternative class of models called recurrent models has also been proposed by taking into account the role of intracortical connections. In the recurrent models, the orientation tuning of the membrane potential evoked by direct inputs from LGN is assumed to be broad; however, this weak tuning is sharpened by the strong intracortical connections. These recurrent models can be divided into two groups depending on the amount of contributions of intracortical excitatory and inhibitory connections [4–7]. The role of the inhibitory connections is proposed to be more important for orientation selectivity in some inhibitory models [4,5] while excitatory connections are considered to be more relevant in other models [6,7].

An interesting feature of cortical dynamics is the synchronization in the response of neurons [8], the understanding of which is regarded as one of the most important problems in the visual cortical system. Gray *et al.* have found stimulus-dependent synchronization of neuronal responses and long-range synchronization of oscillatory responses in the visual cortex [8], which depend on global stimulus properties such as size and continuity. This observation suggests that a sensory part of the brain detects the objects by synchronization of neurons participating in the feature detection and temporal correlation can be exploited to convey information relevant to perceptual grouping. However, until now, little was understood about the mechanism underlying this type of synchronization in connection with the intracortical connections [8], and the relationship between the synchronization and sharp orientation tuning [9] remains largely unknown.

Recently, simulations of dynamic neural network models have attracted much attention as an efficient research tool for understanding the orientation selectivity. The design of the network structures is based on the experimental data and active neuron models with the use of synaptic connections, so these models give more realistic understanding of neural systems than conceptual models. A dynamic neural network model for orientation selectivity was first proposed by Somers *et al.* [7]. They assumed that the visual cortex is composed of columns, where the intracortical connections were determined by the angular difference of the preferred orientations. They also paid attention to the importance of the firing rate averaged over all the excitatory cells within a column. The sharp orientation selectivity was observed in the tuning curve of the ensemble-averaged firing rate. They, however, did not explore the relationship between the orientation selectivity and dynamical states such as synchronization in the neural activities. After the pioneering work of

 ©2004 The American Physical Society

Somers *et al*. [7], many neuronal network models were proposed [9–11]. Hansel and Sompolinsky have studied the relationship between the orientation selectivity and the dynamical phenomena of synchronization in the hypercolumn model. They observed the synchronization in the autocorrelation and cross correlation functions of the cortical cell activities when there is sharp orientation selectivity. However, in their model the columnar structure was absent, so it is hard to specify the collective activity of cells in the same column and synchronization between them. That is, the dynamical properties of averaged neural activity for cells within a column, which we call *columnar activity*, have not been investigated yet. Also, the relations between the orientation selectivity and the dynamical properties of intercolumnar and intracolumnar neural activities remain unclear.

In the present study, a hypercolumn model representing one cycle of preferred orientations is constructed using a network of columns of Hodgkin-Huxley neurons with intracortical short-range excitatory and long-range inhibitory connections under visual stimulus currents. The tuning curves of the firing rate in the model showed sharp orientation selectivity with contrast invariance even though LGN inputs are not tuned sharply. For the dynamical properties of neural activities, firings of excitatory cells in the individual columns are found to be synchronized and the power spectra of the averaged firings of all the excitatory cells in each column are localized around particular frequencies. The peak height of the power spectrum (PHPS), which is calculated from the averaged firing activities within a column, and autocorrelation and cross correlation are introduced to quantify the degree of synchronization. The PHPS as a function of stimulus orientation also shows sharp orientation selectivity as seen in the firing rate, which indicates that the degree of synchronization of firings strongly depends upon the stimulus orientation. When the tuning properties for ensemble-averaged firing activities are investigated as a function of synaptic parameters, we find that there exist appropriate values of intracortical connection strengths, which result in both tight orientation tuning and strong synchronization of firings. Interestingly, it is found that the excitatory coupling strength is balanced with the inhibitory coupling strength in the appropriate coupling strength. The overall properties of tuning are found to be robust for a broad class of neuron models and synaptic models. In Sec. II, a simple neural network model of the hypercolumn is introduced. In Sec. III, we present the results of numerical simulations on orientation selectivity with our model. We end with a summary and discussions.

II. MODELING A HYPERCOLUMN

The network model composed of 15 columns is designed as a hypercolumn model as in Fig. 1(a), where the preferred orientation varies discretely from $-90°$ to $+90°$ with an increment of 12.85°. The network consists of 225 cortical neurons where 45 neurons are inhibitory cells (20%) and 180 neurons excitatory cells (80%) [12]; each column contained 12 excitatory neurons and 3 inhibitory neurons. The model cortical cells either excitatory or inhibitory are given by the Hodgkin-Huxley (HH) neurons [13].

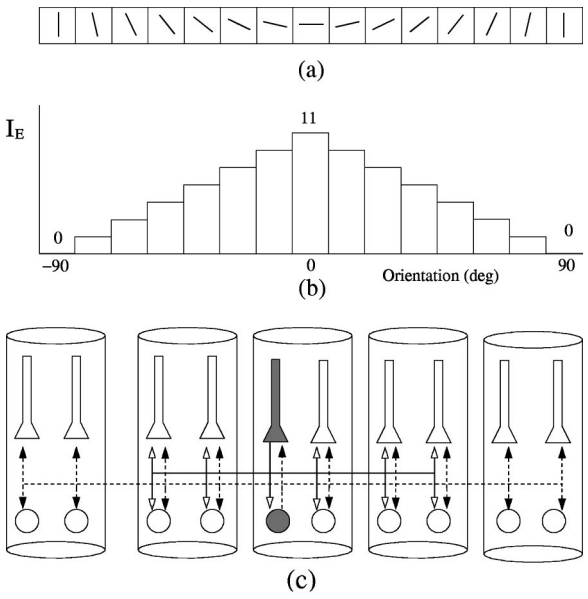

FIG. 1. (a) The preferred orientation and (b) the input stimulus amplitude. The preferred orientation for each column is represented by the angle of each bar in (a) and the input stimulus amplitude by the height of each box in (b). (c) The intracolumnar and intercolumnar lateral connections. The pyramid-shaped figures represent pyramidal cells, the circles inhibitory cells. The excitatory connection from a pyramidal cell (gray) is represented by solid arrows and the inhibitory connection from an inhibitory cell (gray) by dashed arrows.

A simple pattern of the intracortical connections is assumed in this model to be the short-range excitatory and long-range inhibitory [see Fig. 1(c)], as observed in an anatomical study of the cortex [14]. In the model, the excitatory connections are all-to-all inside individual orientation columns or intercolumnar connections between the nearest-neighbor columns. The strength of the intercolumnar connections is 15% of that of the intracolumnar connections. An inhibitory neuron is connected globally to the other neurons in the whole networks. The model proposed here has short-range excitatory and long-range inhibitory connections similar to the structure of connections in the model by Somers *et al.* [7].

A. Hodgkin-Huxley neurons

We adopt the Hodgkin-Huxley neuron as a model of excitatory and inhibitory cells because it has served as a simple and typical paradigm for tonically spiking neurons based on the voltage-dependent nonlinear membrane conductances. The Hodgkin-Huxley neuron model was originally derived from the dynamical behavior of squid giant axons in 1952 [13] and is described by four ordinary differential equations with respect to four variables V, m, n, and h. The membrane potential V_i of the ith neuron in the network is given by Kirchhoff's law of current conservation:

$$C\frac{dV_i}{dt} = I_{ion,i} + I_{E,i} + I_{syn,i} + I_{noise,i}, \tag{1}$$

where C is the membrane capacitance, $I_{E,i}$ the external stimulus current, $I_{ion,i}$ the ionic current through ion channels, $I_{syn,i}$ the synaptic current from the excitatory and inhibitory cells in the columns, and $I_{noise,i}$ the noisy input current. The voltage-dependent ionic current is the sum of currents through the sodium channel (Na), the potassium channel (K), and the leaky current (l):

$$I_{ion,i} = -g_{Na} m^3 h (V_i - V_{Na}) - g_K n^4 (V_i - V_K) - g_l (V_i - V_l), \tag{2}$$

where g's with subscripts Na, K, l are the maximum conductances for individual channels, and V's are the corresponding reversal potentials.

The time-varying gate variables m, h, and n are associated with activation of Na channels, inactivation of Na channels, and activation of K channels, respectively, and obey the following equation:

$$\tau_x(V) \frac{dx}{dt} = x_\infty(V) - x. \tag{3}$$

Here x denotes each of the gate variables, and τ_x and x_∞ are the relaxation time and stationary value of the gate variable, respectively. A more detailed description of these parameters can be obtained from the literature [13,15,16] (see Appendix A).

B. Stimulus currents

When the visual stimulus of a bar is presented with an orientation angle θ_0, the stationary input current to a cell in the ith column through the geniculo-cortical afferent inputs is assumed to be a function of $|\theta_i - \theta_0|$ as $I_{E,i} = F(|\theta_i - \theta_0|)$, where $F(\theta)$ is a decreasing function of θ with a single maximum at $\theta = \theta_0$, and θ_i the preferred orientation of the cell. For simplicity, we assumed a linearly decreasing function with a half width of 45° as in Fig. 1(b). This weakly tuned input current is adopted based on the experimental finding that the tuning profile of the membrane potential driven only by the LGN input was broad with a half width of about 45° [17]. When $\theta_0 = 0°$, the input current is written by

$$I_{E,i} = I_0 c \frac{|90° - |\theta_i||}{90°}, \tag{4}$$

where I_0 is the maximum current for the column with $\theta_i = 0°$, and c the stimulus contrast which takes a value between 0 and 1. The inhibitory cells are assumed to receive the same input current as the excitatory cells in the same column. Here, we assume that $I_{E,i}$ is proportional to the stimulus contrast c for simplicity with $I_0 = 11\ \mu\text{A/cm}^2$ for the maximal stimulus contrast.

The synaptic current $I_{syn,i}(t)$ is typically modeled by the α function [18], which characterizes a quick rise and a slow decay of the post-synaptic potential induced by a spike from a presynaptic neuron. That is, the synaptic current is given by

$$I_{syn,i}(t) = -G_{ex} \sum_{j,k} \alpha(t - t_{j,k})(V_i - V_{ex}) - G_{inh} \sum_{j,l} \alpha(t - t_{j,l})(V_i - V_{inh}), \tag{5}$$

with the α function $\alpha(t) = (t/\tau) e^{-t/\tau}$ specified by the time constant τ. The maximum synaptic conductances and the synaptic reversal potentials are G_{ex} and V_{ex} for the excitatory synaptic current and G_{inh} and V_{inh} for the inhibitory synaptic currents, respectively. The occurrence time $t_{j,k}$ (or $t_{j,l}$) represents the jth spike in the kth (or lth) presynaptic excitatory neuron in the lth inhibitory one. The summation is taken for all the events of action potentials and for all the presynaptic neurons. The time constant, τ, is chosen to be 2 msec for excitatory synapses and 5 msec for inhibitory synapses. We assume that $V_{ex} = -45$ mV for excitatory synapses and $V_{inh} = -80$ mV for inhibitory synapses with the resting membrane potential $V_{rest} = -65$ mV [15,16].

We employ the correlated noisy current with Ornstein-Uhlenbeck (OU) process with the correlation time τ_n:

$$\tau_n \frac{dI_{noise,i}}{dt} = -I_{noise,i} + \sqrt{2D}\,\xi(t), \tag{6}$$

where $\xi(t)$ is the Gaussian white noise, and D the noise intensity. Here, we assume that τ_n is 2 msec [19].

C. Peak height of the power spectrum

Suppose that t_{ij} represents the occurrence time of the jth spike in the ith neuron; then, the spike train h_i of the ith neuron is given by $h_i = \Sigma_j \delta(t - t_{ij})$. To characterize the information processed by the excitatory cells in a column, we adopt the averaged spike train [20,21] $\overline{h} = (1/N)\Sigma_i h_i$, where the index i spans all the excitatory cells in a column, and N represents the number of excitatory cells in a column. The averaged spike train shows periodic and clustered spike activities in the presence of synchronization, whereas it shows a random and irregular sequence of spikes in the absence of synchronization. When the cells show synchronized firings, the power spectrum of the firings is localized around particular frequencies and the peak height is proportional to the degree of synchronization. In practice, this power spectrum is given as the Fourier transformation of the autocorrelation of the averaged spike train. When there occur oscillations by the synchronized activities in the averaged spike train, we can observe periodic peaks in the autocorrelation function. The period of oscillations is given by the inverse of the frequency around which the power is localized. The degree of synchronization of firings in a column is quantified in our study by the PHPS of the averaged spike train $\overline{h}(t)$ [21].

III. NUMERICAL RESULTS

Orientation selectivity has been intensively investigated in the physiological experiments since the pioneering work by Hubel and Wiesel (see, for example, Das [1] and Sompolinsky and Shapley [2]). The firing rate of a simple excitatory

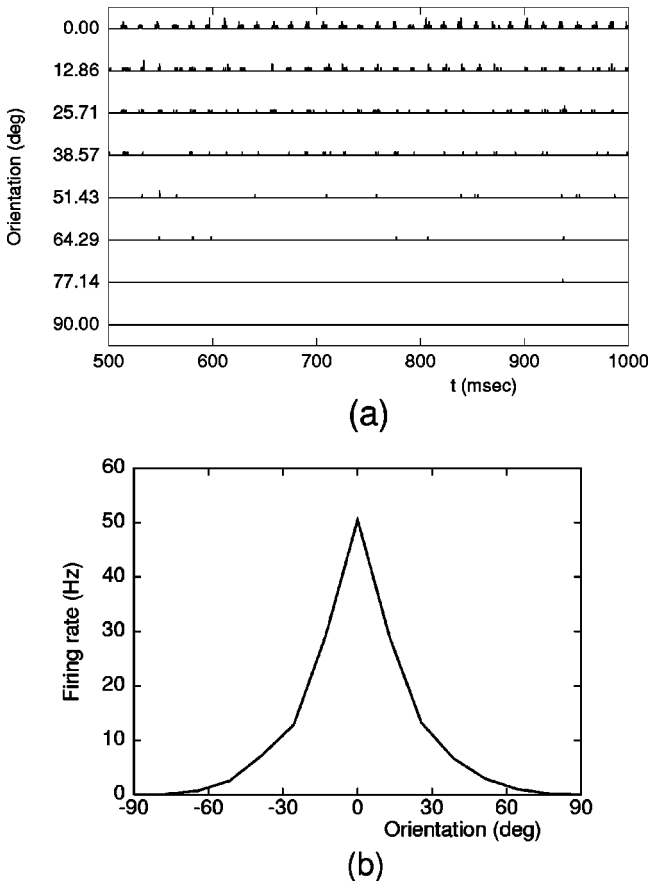

FIG. 2. (a) The averaged spike trains for individual columns of our hypercolumn model and (b) the tuning curve of the average firing rate calculated from the averaged spike trains in (a). These results were obtained for the synaptic coupling strengths $G_{ex}=0.05$, $G_{inh}=0.05$, and weak noise with $D=1$.

cell is measured as a function of the stimulus orientation, called the orientation tuning curve. The response of a cell is the maximum at its preferred orientation and falls off as the stimulus orientation departs from the preferred orientation. The degree of tuning is quantified by the half width at the half maximum (HWHM) of the tuning curve. The HWHM is about 20° for simple cells of the cat visual cortex [22].

We investigate the properties of orientation tuning of cortical cells in our hypercolumn model. A typical example of the averaged spike trains elicited from individual columns is shown in Fig. 2(a). We obtain the orientation tuning curve of the firing rate from the averaged spike trains and depict in Fig. 2(b). The HWHM of the tuning curve is as small as about 18° and this tuning width agrees well with the experimental observations in the cat visual cortex.

The contrast invariance in orientation tuning is another characteristic property of the cortical cells in the primary visual cortex [23,24], which indicates that the sharpness of orientation tuning is nearly unchanged for a broad range of stimulus contrast. We also estimate this property in the proposed hypercolumn model by changing the values of contrast c in Eq. (4). The tuning curves for different values of the stimulus contrast are shown in Fig. 3. We find that all the HWHM remain almost the same in spite of the change in the

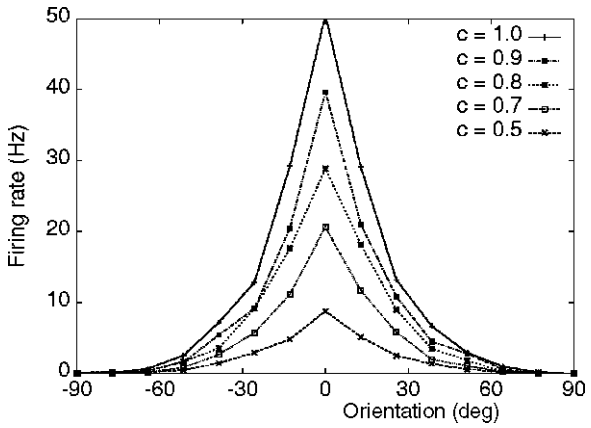

FIG. 3. The average orientation tuning curves obtained from our network for various stimulus contrasts c between 0.5 and 1.0. The simulations were performed for $G_{ex}=0.05$, $G_{inh}=0.05$, and weak noise $D=1$.

strength of the forcing amplitude, which indicates that contrast invariance is achieved as in neuronal responses in the primary visual cortex.

We observe periodically clustered spikes in the averaged spike trains of the individual columns in Fig. 2(a) even though the model cortical cells receive noisy current. We can also see in Fig. 2(a) that the periodic structure of synchronized firings becomes deteriorated as the preferred orientation of the column departs from the stimulus orientation. When we calculate the power spectrum of the spike train for the column with preferred orientation 0°, it has a sharp peak with broad background. As the preferred orientation of a column departs from the stimulus orientation, the PHPS decreases without changes in the background level. We draw the tuning curve of the PHPS against the preferred orientation in Fig. 4. Interestingly, we observe in this tuning curve that the PHPS is slightly sharper than the tuning curve of the firing rate. This finding implies that orientation selectivity in the firing rate is tightly correlated with synchronized firings.

The temporal variability of the activity of a neuron or a column can be measured by calculating the autocorrelation

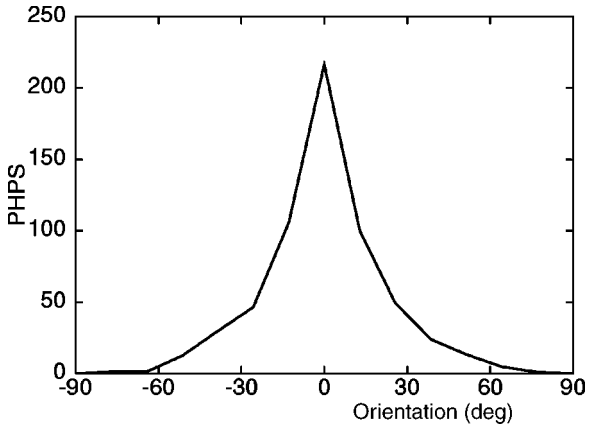

FIG. 4. The tuning curve for the peak height of power spectrum (PHPS). The power spectrum was calculated from the averaged spike trains in Fig. 2(a).

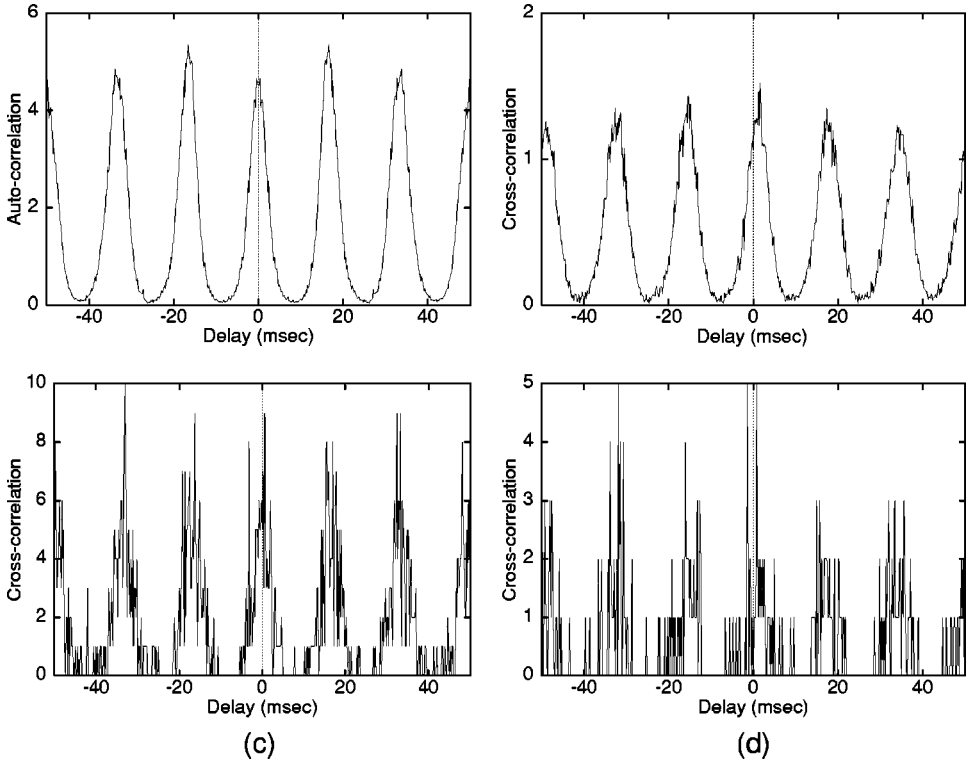

FIG. 5. (a) The autocorrelation function of the spike train of a column with preferred orientation $\theta_1=0°$ and (b) the cross correlation function between the spike trains of two columns with preferred orientation $\theta_1=0°$ and $\theta_2=25.71°$. (c) The cross correlation function between the spike trains of two cells in the same column with preferred orientation $\theta_1=0°$ and (d) the cross correlation function between the spike trains of two cells in the two columns with preferred orientation $\theta_1=0°$ and $\theta_2=25.71°$. The spike trains are obtained from Fig. 2.

function from the individual or averaged spike trains. As is seen in Fig. 5(a) for the population activity, the oscillatory component remains synchronized. The autocorrelation function of an individual spike train shows similar oscillations. The degree of the coherent synchronization between pairs of neurons or columns can be estimated by the cross correlation by using the individual or averaged spike trains. Figure 5(b) shows the cross correlation of the averaged spike trains between two columns. The cross correlation for the individual spike train of two neurons shows similar properties [see Figs. 5(c) and 5(d)]. We observe the shift of the maximum in the cross correlation function from delay $\tau=0$ msec. As the difference of the preferred orientations of two cells or two columns increases, this time delay increases. The shift of the peaks in time is of the order of several msec in our study, as observed in the experiment [25] and the model [9].

To see how much the intracortical connections determine the orientation-selective neuronal responses, we draw the contour plots of the maximal firing rate, which is the averaged firing rate of the column with preferred orientation, $\theta=0°$, and the HWHM in the tuning curve in the two-dimensional parameter space spanned by the excitatory and inhibitory synaptic coupling strength in Fig. 6. The increase in the inhibitory coupling strength reduces the maximal firing rate [see Fig. 6(a)]. Interestingly, the increase in the excitatory coupling strength also reduces the maximal firing rate [see Fig. 6(a)]. It is because the strong excitatory synaptic input during the refractory period delays the time of the successive action potential generation that is proportional to the strength of the excitatory coupling [15,16]. If we assume that active neural responses are more effective in signal processing with relatively larger synaptic current transmission, an appropriate range of the coupling strength for intracortical

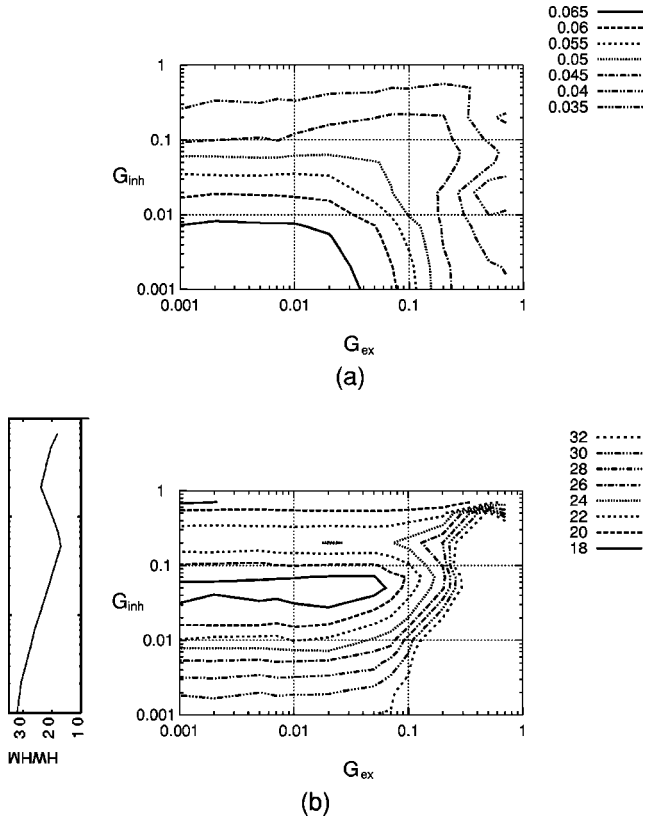

FIG. 6. The contour plots of (a) the maximal firing rate and (b) the half width at half maximum (HWHM) in the parameter space the functions of excitatory and inhibitory coupling strengths for $D=1$. The plot on the left denotes the HWHM for $G_{ex}=0.05$.

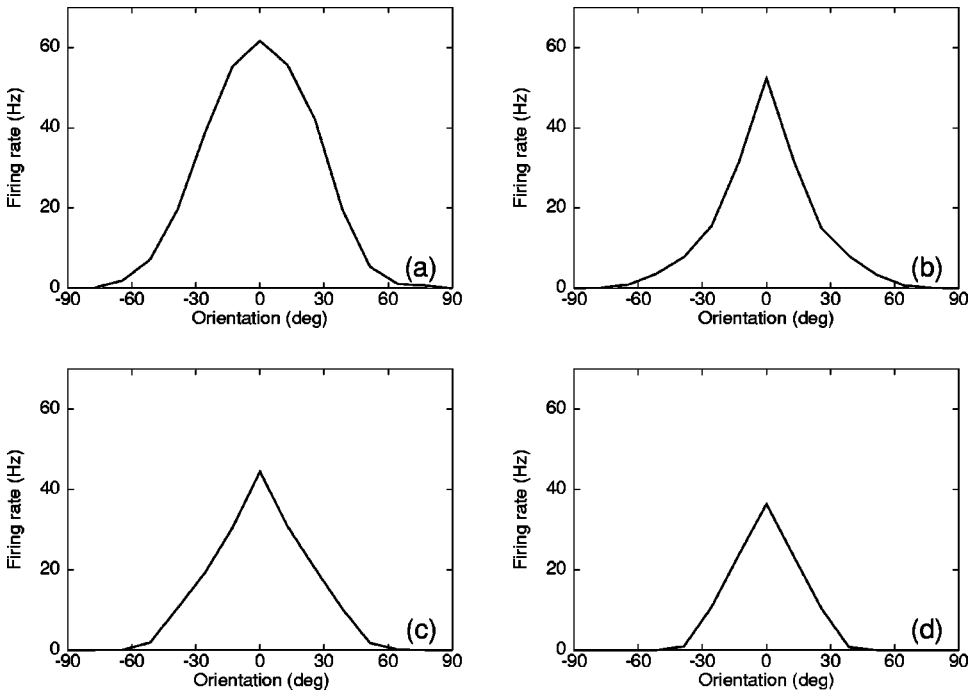

FIG. 7. The tuning curves of averaged firing rates for four different inhibitory coupling strengths: (a) $G_{inh}=0.005$, (b) $G_{inh}=0.05$, (c) $G_{inh}=0.2$, and (d) $G_{inh}=0.7$. The excitatory coupling strength is fixed at $G_{ex}=0.05$.

connections can be estimated as $G_{ex}<0.1$ and $G_{inh}<0.1$.

We find that the width of the orientation tuning also depends upon the synaptic coupling strength of intracortical connections as shown in Fig. 6(b). When the excitatory coupling strength is strong (roughly, $G_{ex}>0.1$), the HWHM becomes larger due to the nonlinear responses of neurons. When the excitatory coupling strength is not so strong (roughly, $G_{ex}<0.1$), the HWHM is determined by the inhibitory coupling only. The HWHM has one minimum near $G_{inh}\sim 0.05$ when the inhibitory coupling is varied from $G_{inh}=0$ to $G_{inh}=0.2$. When $G_{inh}>0.2$, the HWHM decreases monotonically. The mechanisms for the emergence of a minimum can be understood by investigating the change of the tuning curves in Fig. 7 as a function of the inhibitory coupling. When the inhibitory coupling increases to 0.05, the tuning curve becomes sharper due to the decrease of its width by stronger lateral inhibition [compare Fig. 7(a) with 7(b)]. As the inhibitory coupling increases further to $G_{inh}=0.2$, the maximal firing rate—that is, the peak value in the tuning curve—decreases more rapidly than the width [compare Fig. 7(b) with 7(c)]. As we increase the inhibitory coupling further to $G_{inh}=0.7$, the firing rates of all columns decrease uniformly and the HWHM becomes smaller again [compare Fig. 7(c) with 7(d)]. If we assume that the visual cortex works well with stronger neural response and sharp orientation tuning [7], the values of appropriate parameters are estimated as $G_{inh}\sim 0.05$ and $G_{ex}<0.07$ from the two contour plots in Fig. 6. In these measures we cannot specify an appropriate range of the excitatory coupling strength.

We study the situation with strong noise in order to explore how the degree of synchronization depends upon the excitatory coupling strength. The firing rates and PHPS values for the 0° column are calculated for several excitatory coupling strengths with the appropriate inhibitory coupling strength $G_{inh}=0.05$ in Fig. 8. When the excitatory coupling strength increases, the firing rate increases slowly; however, the change is small in the weak-coupling condition ($G_{ex}<0.1$), which implies that the synchronized activities are less perturbed by the strong noise if the excitatory connections are strong. In contrast to the firing rate, the PHPS in the same condition increases rapidly and there are large fluctuations in the PHPS due to strong noise. For stronger coupling ($G_{ex}>0.2$), the time delay in the generation of a subsequent spike, which is induced by strong excitatory current during the refractory period, reduces the firing rate and the degree of synchronization. Highly synchronized activities have been

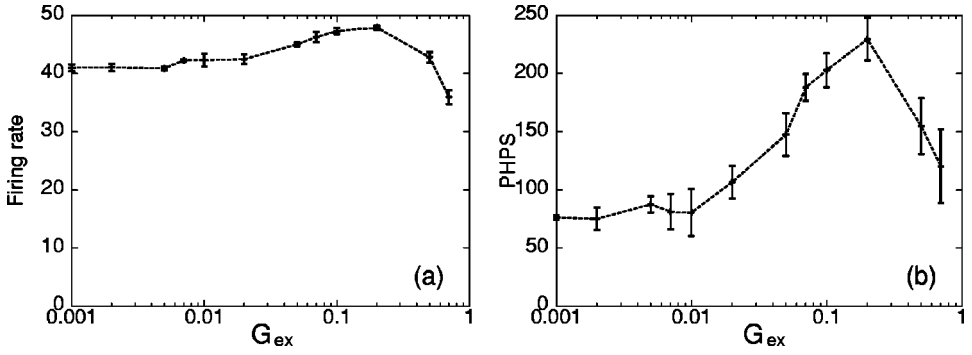

FIG. 8. (a) The firing rates and (b) the PHPS as a function of excitatory coupling strength. The inhibitory coupling strength is $G_{inh}=0.05$ and strong noise is applied with intensity $D=3$. The error bars come from the standard deviation over five trials.

observed in the primary visual cortex in numerous experiments [8]. The appropriate excitatory coupling is estimated as one for maximal PHPS in the regime of weak coupling ($G_{ex}<0.1$). In our study, the appropriate synaptic coupling strength is estimated to be $G_{ex}\sim 0.05$ and $G_{inh}\sim 0.05$ [synaptic currents $\sim O(1)$ μA/cm^2] from Figs. 6(b) and 8(b), respectively. At this appropriate parameter range, the synaptic current evoked by excitatory and inhibitory connections has the same order of magnitude. That is, the excitatory synaptic coupling strengths are balanced with inhibitory synaptic coupling strength at the appropriate parameter range [7].

IV. HYPERCOLUMN MODEL WITH THE MODEL OF CONNOR *et al*

A kind of neural response to the synaptic current observed in the standard Hodgkin-Huxley neuron is called a type-II response; a strong post-synaptic current delays the firing of the next spike, when this current occurs during the refractory period, a short region after action potential. Another type of response is also found; a small excitatory post-synaptic current systematically advances the next spike of the neuron, even when it occurs during the refractory period. This type-I response could be found in an integrate-and-fire neuron and the model of Connor *et al*., which is one of well-known conductance-based models with a spiking nature [26,27]. The study of the dynamical responses and subsequently the tuning properties in the hypercolumn model with models of Connor *et al.* is an interesting problem, because it helps to understand how the network properties such as the orientation tuning may depend on the individual cell property.

A typical example of the averaged spike trains elicited from individual columns is shown in Fig. 9(a) and the orientation tuning curve of the firing rate is shown in Fig. 9(b). We can observe periodically clustered spikes in the averaged spike trains of the individual columns in Fig. 9(a), even though the model cortical cells receive noisy current. The tuning curves in the PHPS have sharp tuning. Interestingly, this strong synchronization disappears even when the synaptic time constant of excitatory synapse $\tau_{ex}=2$ msec, which is relatively small. In the case of the model with the Hodgkin-Huxley neurons, we find the abrupt reduction of synchronization at the larger time constant of $\tau_{ex}\sim 4.0$ msec. This observation implies that the synchronization in the hypercolumn model with the model of Connor *et al*. is more sensitive and fragile. The HWHM of the tuning curve in this study shows sharp orientation tuning as in the hypercolumn model with the Hodgkin-Huxley neuron. The characteristics of tuning curves are not the same: the nonzero firing rate is not observed at the columns with large $|\theta-\theta_0|$ different from the hypercolumn model with Hodgkin-Huxley neurons [compare Fig. 2(b) with 9(b)].

The contour plots of the maximal firing rate and the HWHM in the two-dimensional parameter space of the excitatory and inhibitory synaptic coupling strengths are shown in Figs. 10(a) and 10(b). Note that the increase in the inhibitory coupling strength reduces the maximal firing rate. However, we find that the increase in the excitatory coupling strength increases the maximal firing rate, which is quite

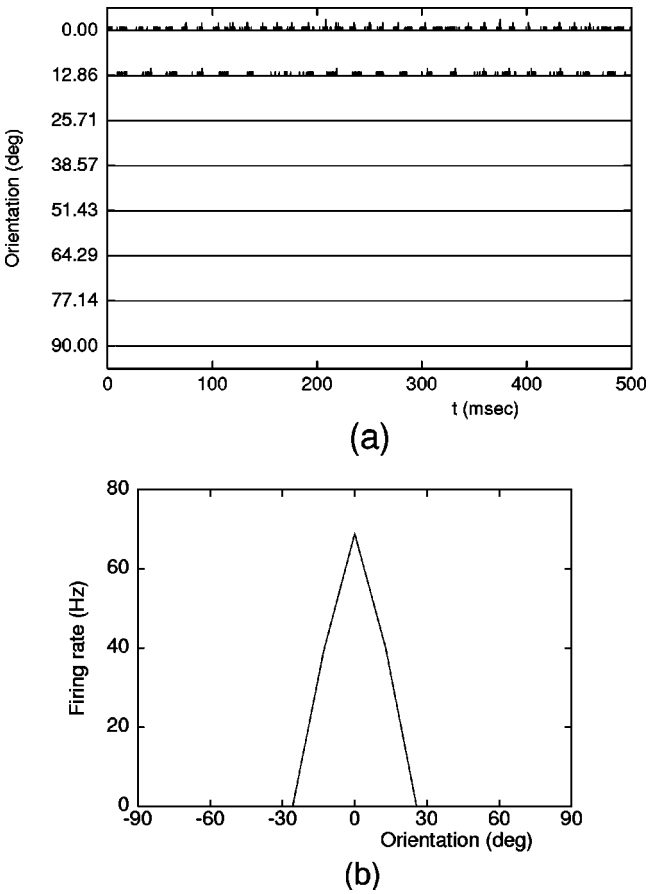

FIG. 9. (a) The averaged spike trains for individual columns of the hypercolumn model with the neural equations of Connor *et al.* and (b) the tuning curve of the average firing rate calculated from the averaged spike trains in (a). These results were obtained for the synaptic coupling strengths $G_{ex}=0.05$, $G_{inh}=0.05$, and weak noise with $D=1$ and $I_E=15$ μA/cm^2. $V_{ex}=0$ mV and $V_{inh}=-85$ mV. The synaptic time constant of excitatory $\tau_{ex}=1$ msec and that of inhibitory $\tau_{inh}=5$ msec.

different from the case with Hodgkin-Huxley neuron. This difference originates from the type-I response property of the model of Connor *et al*. Interestingly, this phase diagram is similar to one by Somers *et al.*, where integrate-and-fire neurons are used. It is due to the fact that the integrate-and-fire neuron is another typical example of neurons with type-I response. In Fig. 10(a), the HWHM of the tuning curves strongly depends upon the inhibitory coupling strength and is nearly independent of the excitatory coupling strength if the coupling strength is not so strong ($G_{ex}<0.1$). This is quite similar to one for the model with the Hodgkin-Huxley neuron. However, there is no minimum in the phase diagram as a function of the inhibitory coupling strength, while the hypercolumn model with the Hodgkin-Huxley neuron showed one minimum with the appropriate coupling strength. The coupling strengths with sharp tuning of 18°, as observed in typical experiments [22], and firing rates of cortical neurons, 40–60 Hz [28], correspond to $G_{ex}\sim 0.03$ and $G_{inh}\sim 0.03$, respectively [29]. The excitatory synaptic coupling strengths are balanced with inhibitory synaptic coupling strength at this parameter range [7].

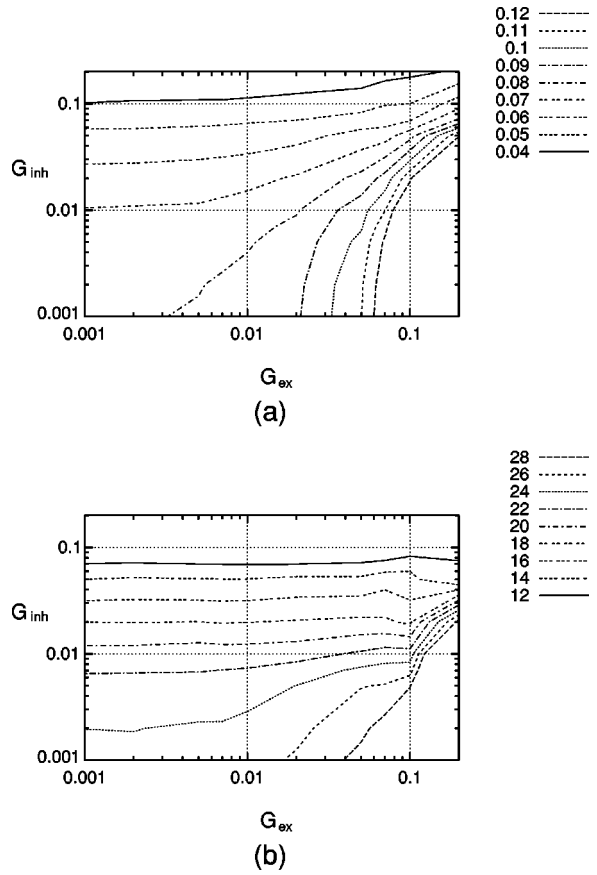

FIG. 10. (a) The contour plots of the maximal firing rate and (b) the HWHM in the parameter space of the excitatory and inhibitory coupling strengths for $D=1$.

V. DISCUSSION

In this paper, the synaptic events are considered as stereotyped waveforms of α functions. An alternative synaptic equation called a kinetic synapse equation is derived by Destexhe *et al.* using a kinetic model [30], which allows more realistic biophysical representations. Tuning properties and the degree of synchronization with this simple kinetic synapse model also show results similar to those in the hypercolumn model with α functions. These results imply that sharp orientation tuning and strong synchronization are consequences of the connection rules of short-range excitation and long-range inhibition and are not much dependent upon the particular model of synaptic interactions.

Another important question is the size dependence of the dynamical phenomena and orientation selectivity. In this paper, several hundreds of neurons are used in the hypercolumn model, which is, however, very small compared with the number of neurons in a real hypercolumn in the cortex. The size dependence of the dynamic behavior of the network is studied as a function of the number of neurons, N, fixing the size of the total synaptic input current I_{syn}. The averaged firing rate and PHPS value of column with $\theta=0$ increase slowly as a function of N as in Figs. 11(a) and 11(b). The HWHM in the tuning curves of firing rates as a function of neuron numbers N are presented in Fig. 11(c). The HWHM do not depend much upon N and exhibit sharp orientation tuning in the large-N limit. Likewise, the HWHM of PHPS as a function of N in Fig. 11(d) also show sharp tuning and strong synchronization in the large-N limit.

We have also studied the dependence of tuning curves on the number of columns in a hypercolumn. Here, the total number of cells in a hypercolumn is fixed. We assume that the connection strength increases in proportion to the number of columns in order that each cell have the same total synaptic connection strength. The tuning curves for the proposed hypercolumn models are shown in Fig. 12, where we used the same integration time intervals (roughly 3 sec). The irregularity in the tuning curve gradually increases as the number of involved columns increases. Thus, there is a lot of irregularity in the tuning curve of hypercolumn model with 128 columns in Fig. 12(d) because the noisy current effect cannot be reduced much in the averaged firing rate for four cells. The overall shape of the tuning curves is similar for all cases and the values of HWHM are roughly about the same in spite of the difference in the number of columns. This fact implies that the tuning property does not depend much on the number of columns considered but on the hypercolumn structure and the connection rule. Note that the PHPS value decreases as the irregularity in the tuning curve increases. We have also explored a different network model with fixed lateral excitatory connection strength for the hypercolumn model with 16, 32, 64, and 128 columns. In this case, we find that the overall shape of all tuning curves is similar for all cases and these tuning curves look similar to those in Fig. 12.

In our hypercolumn model, we tried to make it biologically plausible with a physiological neuron model and cortical column structures. However, we had to make some assumptions to simplify the problem. First, our model focuses only on the activities of cortical cells, excluding the explicit description of LGN structures and neural activities of LGN cells. Instead, it is incorporated into our model in the form of the input current from LGN cells. That is, the sum of synaptic currents from a large number of LGN cells is described as a simple form of input current, which is assumed to be constant with a noisy part. Second, the intracortical networks are short-range excitatory and long-range inhibitory. For simplicity, these excitatory and inhibitory connections are assumed to be global for both individual columns and intercolumnar connections. In a real cortical system, the lateral connections have inhomogeneities. For example, the cortical cells are not connected globally and the synaptic coupling strengths are not identical. The consideration of these inhomogeneities in the lateral connections—for example, through the use of the probabilistic connection rule proposed by Somers *et al.* [7]—can be one possible way to improve our model. Third, we used a Hodgkin-Huxley neuron, which is a paradigm for tonically spiking neurons and much used for studying synchronization phenomena in the cortex. It would be interesting to build the hypercolumn model with more realistic cortical neurons that is based on the experiments on pyramidal cells and inhibitory cells and study detailed properties of orientation selectivity.

In this study, we have built a biologically plausible network for a hypercolumn and investigated dynamical responses of its columnar activities. In the case of Hubel-

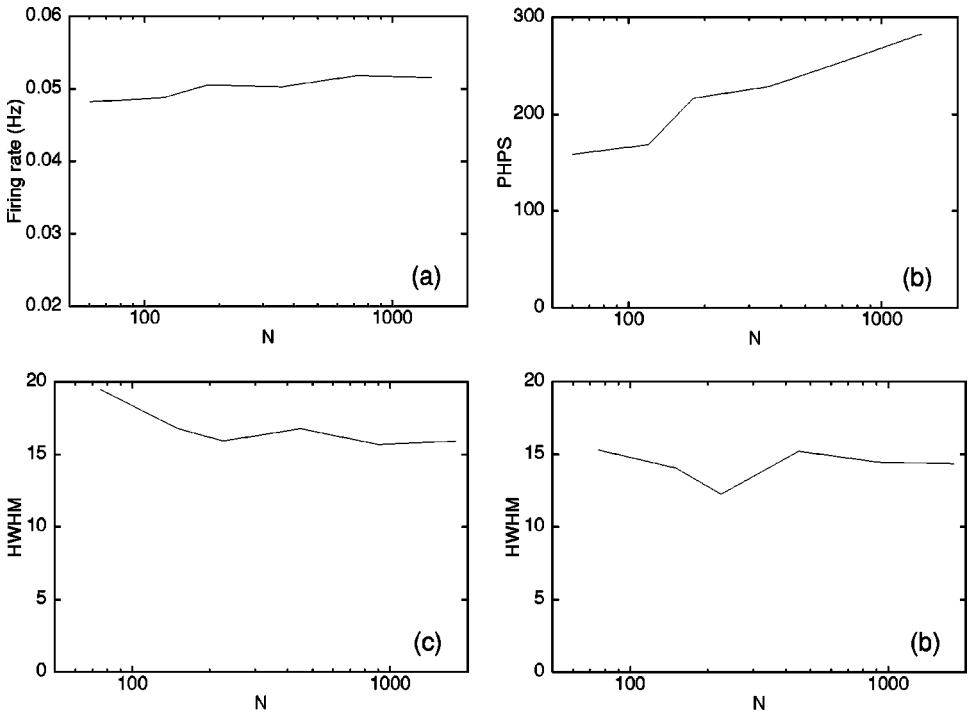

FIG. 11. (a) The plots of the maximal firing rate and (b) maximal PHPS of the column with $\theta=0°$ as a function of the number of neurons N. (c) The plots of the HWHM of the firing rate and (d) HWHM of PHPS as a function of the number of neurons N. Here, we studied $N=75,150,225,450,900,1800$, respectively. These results were obtained for the synaptic coupling strengths $G_{ex}=0.05$, $G_{inh}=0.05$, and weak noise with $D=1$ and $I_E=11\ \mu\mathrm{A/cm}^2$.

Wiesel models [3], the thalamocortical input is assumed to give a main contribution to sharp orientation tuning. In our model the input current is broadly tuned with a half width of 45°. However, the tuning curves of the firing rate of cortical cells still show sharp orientation selectivity due to the sharpening by intracortical connections. The investigation of tuning properties for ensemble-averaged firing activities as a function of synaptic parameters shows that the orientation selectivity depends strongly on the inhibitory coupling strength, while the synchronization in the spike activities of excitatory cells depends on the excitatory coupling strength. Here, the half width of tuning curves is determined by the coupling strength of inhibitory synapses. This suggests that inhibitory coupling plays a key role in sharpening orientation selectivity, which is in line with the previous inhibition dominant models for orientation selectivity [4,5,31].

Our model predicts that the synchronization within a column and the orientation selectivity are correlated strongly. It would be interesting to measure the synchronization within a column through MUA(multi-unit activity) or LFP(local-field potential) instead of a single neural activity. The relationship between the degree of synchronized activities measured by

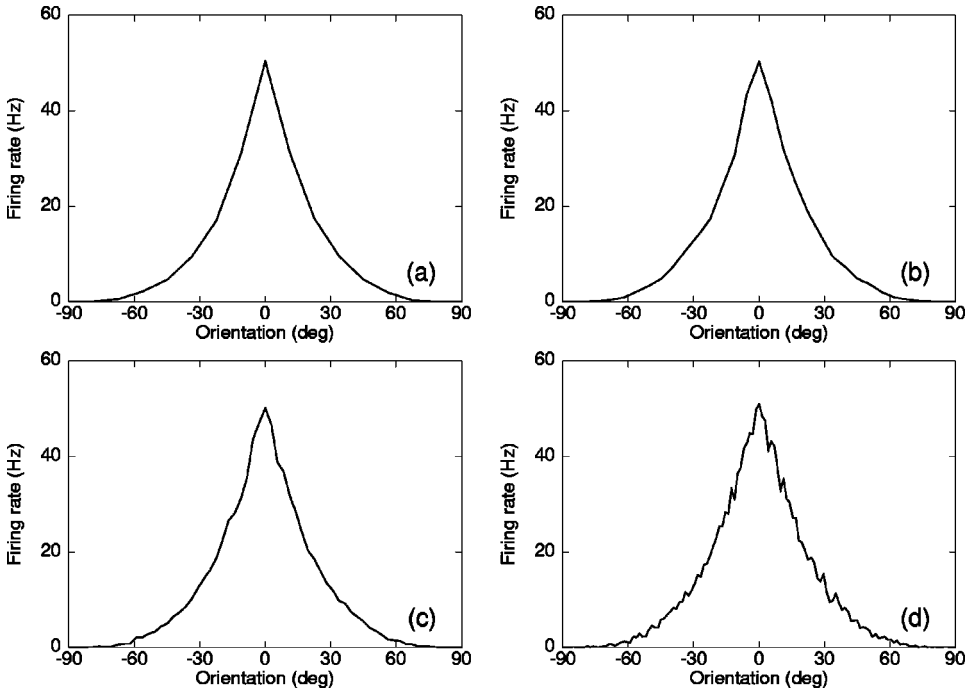

FIG. 12. The tuning curves of averaged firing rates for four different hypercolumns with (a) 16 columns, (b) 32 columns, (c) 64 columns, and (d) 128 columns. The inhibitory coupling strength is fixed at $G_{inh}=0.02$ and the excitatory coupling strength (a) $G_{ex}=0.02$, (b) $G_{ex}=0.04$, (c) $G_{ex}=0.08$, and (d) $G_{ex}=0.16$.

MUA and the tuning curves of firing rate can provide further experimental details for testing and improving our hypercolumn model.

ACKNOWLEDGMENTS

This work was supported by the Ministry of Science & Technology and the Ministry of Education in Korea. A part of this study was performed through Special Coordination Funds of the Ministry of Education, Culture, Sports, Science and Technology, the Japanese Government.

APPENDIX A: HODGKIN-HUXLEY NEURON

The parameters g_{Na}, g_K, and g_l are the maximum conductances per unit surface of the axon for the sodium, potassium, and leakage currents, respectively, V_{Na}, V_K, and V_l are the corresponding reversal potentials, and C is the capacitance per unit surface. For the squid axon, typical values of the parameters at 6.3 °C are $V_{Na}=50$ mV, $V_K=-77$ mV, $V_l=-54.5$ mV, $g_{Na}=120$ mS/cm^2, $g_K=36$ mS/cm^2, $g_l=0.3$ mS/cm^2, and $C=1$ μF/cm^2. The functions $m_\infty(V)$,$h_\infty(V)$, and $n_\infty(V)$ and the characteristic times in milliseconds, τ_m, τ_n, and τ_h, are given as follows: $x_\infty(V)=a_x/(a_x+b_x)$, $\tau_x=1/(a_x+b_x)$ with $x=m,n,h$ and $a_m=0.1\ (V+40)/\{1-\exp[(-V-40)/10]\}$, $b_m=4\exp[(-V-65)/18]$, $a_h=0.07\exp[(-V-65)/20]$, $b_h=1/\{1+\exp[(-V-35)/10]\}$, $a_n=0.01\ (V+55)/(1-\exp[(-V-55)/10)]$, and $b_n=0.125\exp[(-V-65)/80]$.

APPENDIX B: THE MODELS OF CONNOR *et al*

The Hodgkin-Huxley equations for a space-clamped squid axon have been modified to approximate voltage clamp data from repetitive-firing crustacean walking leg axons. This model incorporates, in addition to the sodium and delayed rectifier potassium currents of the Hodgkin-Huxley neuron, an A current. The equation for the sodium and potassium currents in the model of Connor *et al.* is the same with the Hodgkin-Huxley neuron with different parameters. In the model of Connor *et al.* typical values of the parameters are [26,27] $V_{Na}=55$ mV, $V_K=-72$ mV, $V_l=-17$ mV, $g_{Na}=120$ mS/cm^2, $g_K=20$ mS/cm^2, $g_l=0.3$ mS/cm^2, and $C=1$ μF/cm^2. The functions $m_\infty(V)$, $h_\infty(V)$, and $n_\infty(V)$ and the characteristic times in milliseconds, τ_m, τ_n, and τ_h, are given as follows: $x_\infty(V)=a_x/(a_x+b_x)$, $\tau_x=c_x/3.8(a_x+b_x)$ with $x=m,n,h$ and $c_m=c_h=1$ and $c_n=2$, and $a_m=0.1\ (V+29.7)/\{1-\exp[(-V-29.7)/10]\}$, $b_m=4\exp[(-V-54.7)/18]$, $a_h=0.07\exp[(-V-48)/20]$, $b_h=1/\{1+\exp[(-V-18)/10]\}$, $a_n=0.01\ (V-45.7)/\{1-\exp[(-V-45.7)/10]\}$, and $b_n=0.125\exp[(-V-55.7)/80]$. The A current is described in different way:

$$I_A=-g_A(V-V_A)A^3B,$$

$$\frac{dA}{dt}=\frac{A_\infty(V)-A}{\tau_A(V)},$$

$$\frac{dB}{dt}=\frac{B_\infty(V)-B}{\tau_B(V)},$$

where

$$A_\infty=\left[0.0761\frac{\exp[(V+94.22)/31.84]}{1+\exp[(V+1.17)/28.93]}\right)^{1/3},$$

$$\tau_A=0.3632+\frac{1.158}{1+\exp[(V+55.96)/20.12]},$$

$$B_\infty=\frac{1}{\{1+\exp[(V+53.3)/14.54]\}^4},$$

$$\tau_B=1.24+\frac{2.678}{1+\exp[(V+50)/16.02]}.$$

[1] A. Das, Neuron **16**, 477 (1996).

[2] H. Sompolinsky and R. Shapley, Curr. Opin. Neurobiol. **7**, 514 (1997).

[3] D.H. Hubel and T.N. Wiesel, J. Physiol. (London) **160**, 106 (1962).

[4] A.M. Sillito, J. Physiol. (London) **289**, 33 (1979); A.M. Sillito, J.A. Kemp, and N. Berardi, Brain Res. **194**, 517 (1980).

[5] T. Tsumoto, W. Eckart, and O.D. Creutzfeldt, Exp. Brain Res. **34**, 351 (1979).

[6] R. Douglas, K.A.C. Martin, and D. Whitteridge, J. Physiol. (London) **440**, 659 (1991).

[7] D.C. Somers, S.B. Nelson, and M. Sur, J. Neurosci. **15**, 5448 (1995).

[8] C.M. Gray, P. König, A.K. Engel, and W. Singer, Nature (London) **338**, 334 (1989); C. Gray and W. Singer, Soc. Neurosci. Abstracts **13**, 404 (1987); C. Gray and W. Singer, Proc. Natl. Acad. Sci. U.S.A. **86**, 1698 (1989); B. Jagadeesh, C.M. Gray, and D. Ferster, Science **257**, 552 (1992).

[9] D. Hansel and H. Sompolinsky, J. Comput. Neurosci. **3**, 7 (1996).

[10] T.W. Troyer, A.E. Krukowski, N.J. Priebe, and K.D. Miller, J. Neurosci. **18**, 5908 (1998).

[11] M.C. Pugh, D.L. Ringach, R. Shapley, and M.J. Shelley, J. Comput. Neurosci. **8**, 143 (2000).

[12] P.L.A. Gabbott and P. Somogyi, Exp. Brain Res. **61**, 323 (1986).

[13] A.L. Hodgkin and A.F. Huxley, J. Physiol. (London) **117**, 500 (1952).

[14] J.S. Lund, Q. Wu, and J.B. Levitt, *The Handbook of Brain Theory and Neural Networks*, edited by M.A. Arbib (MIT Press, Cambridge, MA, 1995), pp. 1016–1021.

[15] D. Hansel, G. Mato, and C. Meunier, Europhys. Lett. **23**, 367 (1993).

[16] S. Lee, S. Kim, and H. Kook, Int. J. Bifurcation Chaos Appl. Sci. Eng. **7**, 889 (1997).

[17] D. Ferster, C. Sooyoung, and H. Wheat, Nature (London) **380**, 249 (1996).

[18] J.J.B. Jack, D. Noble, and R.W. Tsien, *Electrical Current Flow in Excitable Cells* (Clarendon, Oxford, 1975).
[19] S. Lee, A. Neiman, and S. Kim, Phys. Rev. E **57**, 3292 (1998).
[20] M. Tsodyks, I. Mitkov, and H. Sompolinsky, Phys. Rev. Lett. **71**, 1280 (1993).
[21] W. Rappel and A. Karma, Phys. Rev. Lett. **77**, 3256 (1996).
[22] G.A. Orban, *Neuronal Operations in the Visual Cortex* (MIT Press, Cambridge, MA, 1984).
[23] G. Sclar and R. Freeman, Exp. Brain Res. **46**, 457 (1982).
[24] B. Skottun, A. Bradley, G. Sclar, I. Ohzawa, and R. Freeman, J. Neurophysiol. **57**, 773 (1987).
[25] P. König, A.K. Engel, P.R. Roelfsema, and W. Singer, Neural Comput. **7**, 469 (1995).
[26] J.A. Connor, D. Walter, and R. McKown, Biophys. J. **18**, 81 (1977).
[27] D. Hansel, G. Mato, and C. Meunier, Neural Comput. **7**, 307 (1995).
[28] C.M. Gray, A.K. Engel, P. König, and W. Singer, in *Nonlinear Dynamics and Neuronal Networks*, edited by H.G. Schuster (VCH, New York, 1991), pp. 27–55.
[29] S. Lee and S. Kim, Phys. Rev. E **60**, 826 (1999).
[30] A. Destexhe, Z.F. Mainen, and T.J. Sejnowski, Neural Comput. **6**, 14 (1994).
[31] F. Wörgötter, in *Cerebral Cortex*, edited by P. Uliniski (Kluwer Academic/Plenum, New York, 1999), pp. 201–249.